International Journal of Innovative
Computing, Information and Control
Volume **15**, Number **4**, August **2019**

 ISSN 1349-4198
pp. 1581–1589

A NOVEL CLASSIFICATION & REPAIRING FRAMEWORK FOR IRREGULAR MODEL RECONSTRUCTION USING MASS POINT CLOUDS BASED ON FUZZY INFERENCE

Yanju Liu, Huiyu Zhang, Cheng Li, Honglie Zhang and Jiaxing Liu

College of Computer and Control Engineering
Qiqihar University
No. 42, Wenhua Street, Jianhua District, Qiqihar 161006, P. R. China
15146692464@163.com

Received August 2018; revised December 2018

Abstract. *Mass point clouds of irregular model obtained from laser scanner are incomplete, which causes the problem that affects surface reconstruction and subsequent application. Due to the fact that geometry feature of irregular model local area has uncertainty, it is difficult to adopt one effective method to repair the lost data of model. In this paper, point clouds of irregular model are meshed firstly. According to the shape of the boundary, the hole is divided into different types by fuzzy inference system (FIS). Then the corresponding repairing method is presented for each type. For these repairing methods, public modules are introduced in detail. The repairing effect is improved greatly for corresponding methods are carried out to repair hole with different shapes. Experimental results show that the efficiency and accuracy of dental models are improved by the proposed classification and repairing framework effectively.*
Keywords: Mass point clouds, Fuzzy inference system, Irregular model reconstruction, Type of hole, Classification & repairing

1. **Introduction.** The application of irregular model reconstruction is widely used in all kinds of fields. The hole is always formed during the process of reconstruction due to the device itself and technical limitations. Because the laser beam is blocked by some parts of the model, some surface information cannot be directly captured and some grid data are missing. In practical setups, the results often cause defects which restrict its direct application in subsequent automated analysis. Repairing these defects has to be completed prior to applying the mesh generated in further analysis. Existing methods can only repair a certain type of model. At present, there is no universal method for repairing holes in all kinds of irregular models. Filling a complex hole over an irregular area is much more challenging and the behavior of the front is unpredictable, particularly cases which fronts with large curvature disparity rendezvous. Moreover, ensuring non-intersecting face insertion is more cumbersome as the front grows. In the paper, a novel classifying and repairing framework for irregular model is proposed. Holes with different shapes are classified and different types of holes correspond to different repairing methods. Therefore, the holes in the irregular model with different geometry features can be repaired.

The remainder of the paper is organized as follows. In Section 2, related works about repairing holes in irregular models and classification model shapes are analyzed. The boundary of hole is iterated in Section 3. In Sections 4 and 5, the classification and the repairing of hole are presented, respectively. In Section 6, simulation experiments

DOI: 10.24507/ijicic.15.04.1581

are carried out, and the results are analyzed. Finally, conclusions are given with the importance and practical value of the classification and repairing strategy.

2. **Related Works.** Many scholars have studied the vulnerability repairing algorithms deeply and put forward many effective algorithms. The existing repairing methods can be roughly divided into image inpainting method and mesh repairing method. For image inpainting method where multiple views are available, view interpolation can fill most of the holes by using image and depth features from multiple views. Buyssens et al. [1] have modified the filling priority and the patch selection process with the depth information. Foreground removal approach alleviates the foreground loss [2] by detecting and removing the foreground objects. Ciotta and Androutsos [3] have added depth information to improve the quality of image completion results. Howard et al. [4] have exploited depth information to fill the hole area left by unwanted objects in stereo images. The image inpainting method based on above methods handles each frame of the video separately without considering the temporal consistency. Moreover, some trusted textures appearing in other frames may not be recovered as only the current frame is employed to fill the hole. To keep away flicker noise between adjacent frames in the synthesized video, some spatio-temporal approaches extend the image inpainting to fill the hole area with both spatial and temporal consistency. Kim et al. [5] have extended MRF-based inpainting method by additionally adding temporal consistency term to the energy function. Although these spatio-temporal approaches consider the neighboring consistency, the trusted texture might not be recovered without exploiting the total temporal information from all other frames. Li et al. [6] have exploited a new framework to reduce the hole from all possible views. Multiple reference views can largely reduce the holes, but it requires more capturing resources and higher transmission bandwidth than single views.

Mesh repairing method is carried out on the model surface directly. The surrounding area of the hole is searched firstly. According to the mesh, vertex data and features around the hole, a new mesh is inserted to complete the hole. Horkaew and Sinthanayothin [7] have proposed a mesh pre-processing technique, which is the projection of curvilinear non-planar two-manifold hole on a low distortion contour, upon which a network of regular facets may be re-triangulated. The improved method is interactive and knotted case. Fortes et al. [8] have determined method to fill the hole corresponding to shape feature of 3D model. The shape of the original surface is filled by inheritance as much as possible. And patch filling is established for the known figure to realize the repairing of the whole hole. However, requirements of this method are high on the characteristic of hole. When the equipment has low cost or the researcher has high requirements on the scanning speed, the image recognition obtained by the device scanning is not high. Centin et al. [9] have linked the constructed surface of the hole area to the original model naturally by Poisson drive repairing method. However, it is difficult to recover the detailed features of the hole area well. Harary et al. [10] have divided the hole repairing work into two steps. First, the mesh is constructed based on model surface, and then the geometric details are added on the mesh of surface. Sahay and Rajagopalan [11] have repaired the hole in the 3D model by searching similar area. For the method, if there is an area similar to the hole in the model, a better result can be obtained. However, if the hole of the model is unique, it may be distorted or even wrong repairing result is obtained. At the same time, the time complexity of the hole repairing method is often high and it is difficult to repair the complex model effectively. Aiming at the diversity of hole shape and the uniqueness of hole repairing method, the corresponding repairing strategy is presented for the holes with different shapes in this paper. Based on fuzzy inference system (FIS) [12], an idea

that the hole is divided into different types and is repaired correspondingly is proposed. However, how to repair each type of hole is not presented in detail.

3. **Hole Boundary Determination of the Irregular Model.** There are two difficulties in repairing hole during the irregular model reconstruction. One is how to extract hole boundary, and the other is how to obtain information from the hole boundary in order to recover geometry features of original shape as much as possible. The steps of repairing are hole boundary determination, classification of irregular hole according to the shape of hole boundary and repairing hole with different shapes using corresponding method. For mass point clouds of model, it is difficult to determine whether a vertex is on the hole boundary or not, although it is relatively easy to identify the mesh edge. Mesh generated by mass point clouds is adopted. In this section, hole boundary of the irregular model is determined. Some definitions are illustrated as follows.

Definition 3.1. Boundary edge. *For mesh of irregular model, if an edge of mesh belongs to one triangular mesh, then the edge is one of the hole boundaries, and it is called boundary edge.*

Definition 3.2. Inner edge. *For mesh of irregular model, if an edge of mesh belongs to two triangular meshes, it is called inner edge. It is the necessary consistency of surface and has geometry feature.*

Definition 3.3. Hole boundary. *The space polygon formed by boundary edges from end to end is called hole. Because of the complexity of model and uncertainty of lost data, the difficulty of repairing hole is high on shape and size.*

For the mesh of irregular model, hole boundary can be automatically traversed by topological relations. The main idea is that a boundary is firstly found to be a seed edge, and then an adjacent boundary is found. The adjacent boundary is tested to determine whether it is boundary edge or inner edge. If it is inner edge, it is ignored. If it is boundary edge, it is regarded as the new seed edge. The process is repeated, and a closed loop can ultimately be found, as shown in Figure 1. In this way, hole boundaries can be determined.

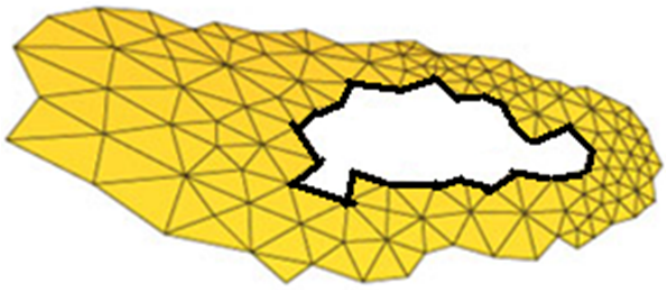

FIGURE 1. Hole boundaries

4. **Classification of Irregular Hole by FIS.** Because of the complexity of irregular hole, many factors must be considered, which makes it difficult to express the filling process in one mathematical function. Therefore, some experiences must be contained in these factors and expressed by FIS. FIS [12] includes four main components: fuzzifier, fuzzy rule base, fuzzy inference engine, and defuzzifier. Classification method of irregular hole using FIS is described in the following part of this section.

4.1. **Fuzzifier of FIS.** Many factors must be considered to repair the incomplete irregular model, including gradient, curvature change rate, k-nearest neighbor (KNN) distance, and normal.

In order to simplify the computations, the triangulation membership function is adopted. And some experiences are added to each domain. The average distance x_{knn} between two vertices for irregular model is 0.005 that reflects our finding and experience. The value of angle e_{normal} for the positive of the normal is 90°, where value of $e_{normal} \in (0°, 90°]$ denotes that the shape of the local area is convex, and value of $e_{normal} \in (90°, 180°)$ denotes that the shape of the local area is concave. The angle of the edge is projected on plane named e_{G3}. e_{G3} can be given to express the geometry feature of the hole, which is divided into four conditions, including $(0°, 90°]$, $(90°, 135°]$, $(135°, 200°]$ and $(200°, 360°]$.

4.2. **Fuzzy rule base of FIS.** These rules mainly stem from our experience and measurement in practice. Mass point clouds of irregular model are formed triangular mesh. Three input variables are firstly input into FIS and fuzzied, which allows the types of hole to be inferred by FIS according to the data fuzzied. The key to inference engine is the collection of fuzzy IF-THEN rules that are set using human experiments. The fuzzy rule Rj is defined as follows:

Rj: if x^i_{knn}, e^{ij}_{normal}, e^{ij}_{G3} then y

where input $= \left[x^i_{knn}, e^{ij}_{normal}, e^{ij}_{G3}\right]^T$ and y are the input vector and output value of FIS, respectively.

Many irregular models with incomplete point clouds are analyzed in our study and the domain of input variables including x^i_{knn}, e^{ij}_{normal} and e^{ij}_{G3} can be expressed the geometry feature of the hole. x^i_{knn} is used to identify the size of the hole, which is computed by a multiple of the average distance in the data, e^{ij}_{normal} is used to determine the sharp feature between neighbor edges, and e^{ij}_{G3} is used to determine the angle projected between edge e_i and edge e_j. The three variables belong to different values that constitute the fuzzy rule base.

4.3. **Defuzzifier of FIS.** The defuzzifier of FIS refers to the type of the hole. There are five types to be divided, including simple-small hole [0 0 0], smooth-ring hole [0 0 1], smooth-island hole [0 1 0], convex-concave ring hole [0 1 1], and complex-island hole [1 0 0]. For different types of the hole, corresponding repairing method is given in the next section.

5. **Repairing Frame for Complex Irregular Holes.** In order to simplify the repairing process and recover the surface feature of irregular model, holes are divided into different types by FIS and given corresponding repairing strategy in Algorithm 1. From Algorithm 1, these different repairing methods are involved in public modules, such as adding new vertex, recovering geometry feature and stitching mesh. Three modules are illustrated in detail.

5.1. **Adding new vertex.** The degree of the minimum angle has been divided into four cases in Figure 2.

In Figure 2(a), $\theta \in (0°, 90°]$. The adjacent vertices of the adjacent edges are connected directly, and new triangular mesh $\Delta A_{i-1}A_iA_{i+1}$ is generated. In Figure 2(b), $\theta \in (90°, 135°]$. A vertex P_1 is added to the plane with $A_{i-1}A_i$, and A_{i+1}, where $|A_iP_1| = (|A_{i+1}A_i| + |A_{i-1}A_i|)/2$, A_iP_1 is angle bisector of $\angle A_{i-1}A_iA_{i+1}$, and two new triangular meshes $\Delta A_{i-1}P_1A_i$ and $\Delta A_iP_1A_{i+1}$ are generated. In Figure 2(c), $\theta \in (135°, 200°]$. Vertices P_1 and P_2 are added to the plane with A_{i-1}, A_i and A_{i+1}, where $|A_iP_1| = |A_iP_2| =$

Algorithm 1 Repairing of Hole by FIS

Input x_{knn}, e_{normal}, e_{G3} to FIS
The output y of FIS
Do case y
Case [0 0 0]: repair it by a plane
Case [0 0 1]: repair it by implicit function
Case [0 1 0]: Add new vertex along the boundary of hole
Add new vertex along the island
Stitch the mesh
Recover feature of hole
Case [0 1 1]: Add new vertex along the boundary of hole
Recover feature of hole
Stitch the mesh
Recover feature of hole
Case [1 0 0]: Add new vertex along the boundary of hole
Recover feature of hole
Add new vertex along the island
Recover feature of hole
Stitch the mesh
Recover feature of hole

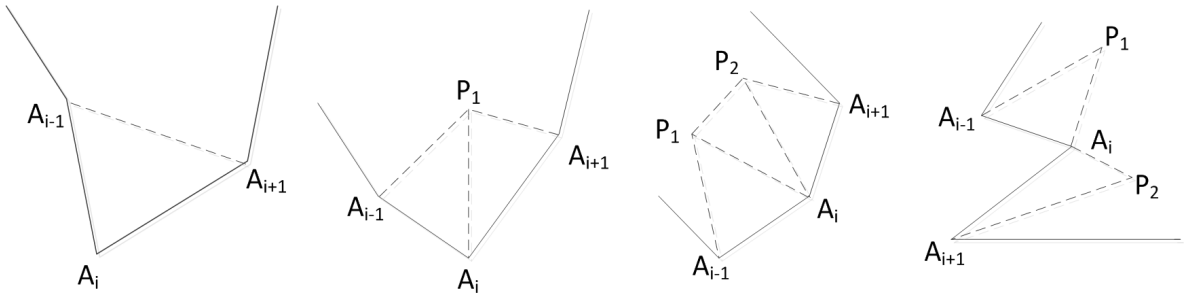

FIGURE 2. New vertex addition for different angles

$(|A_{i+1}A_i| + |A_{i-1}A_i|)/2$. A_iP_1 and A_iP_2 are trisectrices of $\angle A_{i-1}A_iA_{i+1}$, and three new triangular meshes $\Delta A_{i-1}P_1A_i$, $\Delta A_iP_2A_{i+1}$ and $\Delta P_1P_2A_i$ are generated. In Figure 2(d), $\theta \in (200°, 360°]$. Vertices P_1 and P_2 are added to the plane with A_{i-1}, A_i and A_{i+1}. The new equilateral triangular meshes $\Delta A_{i-1}P_1A_i$ and $\Delta A_iP_2A_{i+1}$ are generated.

5.2. **Recovering feature of hole.** In order to recover the geometry features of irregular model, the normal of the new triangular meshes must be adjusted. In essence, this means mapping the new triangle vertex to the 3D surface. The normal of the new triangular mesh is calculated according to the current triangular surface, and its surrounding surface is the boundary mesh of the hole. In this way, complex holes can be repaired in two steps. First, new vertices are added to form a triangular mesh on a plane. Then, the convex-concave feature of the surface is restored by calculating the normal.

The grid surface of each vertex is calculated sharp value, which is described in detail as follows. Normal n of total grid surface is calculated in Equation (1).

$$n = n_f + \sum_{f_j \in N} n_{f_j} \tag{1}$$

where n_f is normal of current triangular surface f, n_{f_j} is normal of surrounding surface f_j, $\{N\}$ is neighbor set of surrounding surface f in Figure 3, and $N = \{f_j | f_j$ is neighbor triangular surface of f, $j = 1, 2, \ldots\}$.

Then, sharp value V_f of surface f is calculated in Equation (2).

$$V_f = \frac{1}{\|N\|} \sum_{f_j \in N} (\varphi_j - \varphi^n)^2 \tag{2}$$

where φ_j is cosine of vectorial angle between n_f and n_{f_j} in Equation (3), $\varphi^n = \varphi(n_f, n)$, and $\|N\|$ is number in $\{N\}$.

$$\varphi_j = \varphi(n_f, n_{f_j}) = \cos(\angle(n_f, n_{f_j})) \tag{3}$$

where $\varphi_j \in [0, 1]$. At the edge or corner of grid surface, φ_j becomes larger, and normal intersection angle of surface has larger sharp value as well.

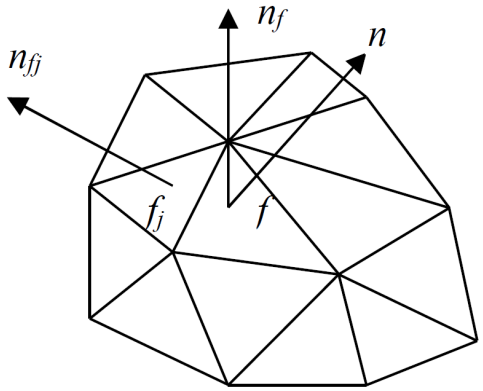

FIGURE 3. Neighbors of surface f

5.3. **Stitching mesh.** The objective of mergence is to determine the corresponding relationship between the boundary vertices generated by the hole and the border vertices of surface mesh model. And then, the corresponding vertices are merged and each border vertex in hole mesh is connected to the boundary vertices around mesh. Set b_i and b_{i+1} to be boundary vertices of the original adjacent mesh. p_k is the boundary vertex of the repaired hole surface mesh. There are three cases in the processing of connecting mesh in Figure 4.

(a) If b_i and b_{i+1} correspond to p_k at the same time, then the three vertices are merged into one vertex.

(b) If b_i and b_{i+1} correspond to p_k and p_{k+1} respectively, and p_k and p_{k+1} are adjacent vertices, then b_i and p_k are merged while b_{i+1} and p_{k+1} are merged as well.

(c) If b_i and b_{i+1} correspond to p_k and p_{k+n} respectively, the vertex p_j between p_k and p_{k+n} is merged with p_k or p_{k+n}. If $|p_j p_k| < |p_j p_{k+n}|$, then p_j is merged with p_k, else p_j is merged with p_{k+n}. The process is not halted until there are only two vertices left. And then b_i and p_k are merged, and b_{i+1} and p_{k+n} are merged as well.

6. **Simulation.** A simulation is conducted to evaluate the performance of the proposed fuzzy inference hole repairing method using dental point clouds. The mass point clouds are from 3D laser scanner, PICZA LPX-250. The number of the scanned teeth is 48921, 48103, 47148 for molar without part crown, molar without part occlusal and canine without tip or side in Figure 5, respectively. The implementation above is carried out using a PC equipped with an Intel Core (TM)i5-4460 processor, 3.20GHz, and 8GB main memory.

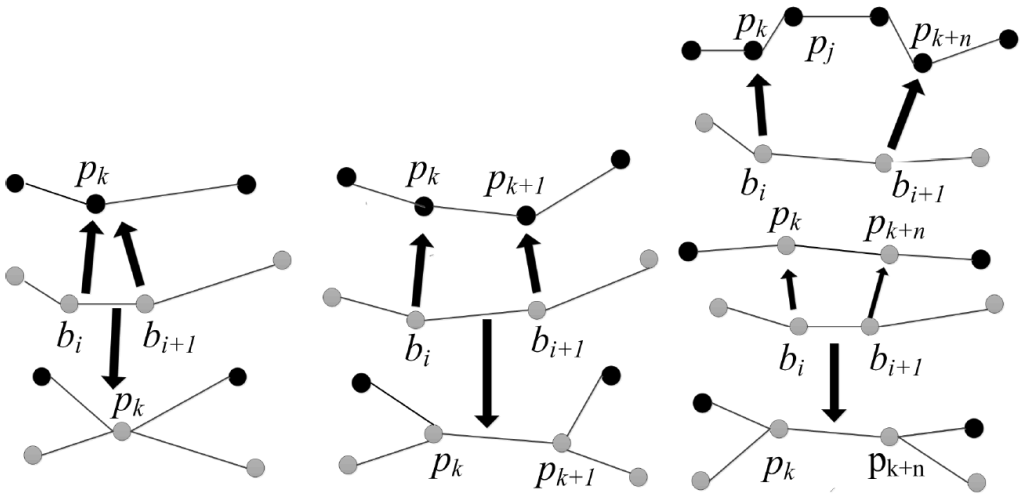

FIGURE 4. Three cases of mesh stitching

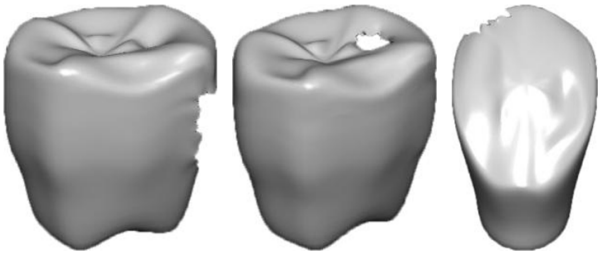

FIGURE 5. Original teeth with hole

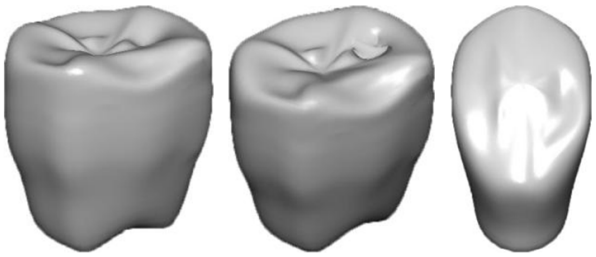

FIGURE 6. Repaired teeth

These models with incomplete point clouds are input FIS respectively. The output of FIS are that the original model of molar without part crown belongs to [0 0 1], molar without part occlusal belongs to convex-concave ring [0 1 1], and canine without tip or side belongs to complex island [1 0 0]. Applying corresponding repairing method, they are repaired in Figure 6.

Horhaew and Sinthanayothin's algorithm [7] and Harary et al.'s algorithm [10] are compared with the proposed algorithm of the paper. The result of comparison is shown that the proposed method outperforms the existing methods. The execution time (s) of our classification strategy is compared with those of the established methods described above in Table 1. In the case of complex holes without any user intervention, the proposed algorithm performs even in only seconds. In situations with incomplete dental information, half of the total time can be saved by classification with FIS. The reconstructed

TABLE 1. Execution time (s) and mean variance (mm) of repaired model are compared with those of Horhaew and Sinthanayothin's and Harary et al.'s

Model	Horhaew and Sinthanayothin's		Harary et al.'s		Proposed	
	Time	Mean variance	Time	Mean variance	Time	Mean variance
Molar without part crown	21.26	0.13	20.37	0.03	19.98	0.01
Molar without part occlusal	29.90	0.26	31.21	0.05	21.32	0.04
Canine without tip or side	42.56	0.09	44.13	0.03	22.64	0.02

models are matched with the original corresponding models in the same world coordinate system by iterative closest point (ICP) algorithm. The mean variance of point position which is listed in Table 1 is regarded as the precision index. The value of mean variance of the proposed algorithm illustrates that the geometry feature of original model can be recovered well. And the value of Harary et al.'s algorithm is close to ours in the precision. On the contrary, the precision of Horhaew and Sinthanayothin's algorithm is poor when no user intervene. The more irregular the teeth is, the more time and accuracy can be improved during the process of repairing. Because FIS can classify the type of dental hole, each type can be repaired by corresponding strategy. Existing methods can repair only one type of hole effectively, and much more time is consumed to repair other types and the precision of reconstruction model is poor.

7. **Conclusions.** For irregular models, a framework for classifying and repairing the hole based on fuzzy inference is proposed which can incorporate experience and distinguish holes in detail. Based on the types of the hole, different repairing strategies can be adopted, and the strategies involve adding new vertex and adjusting the position of vertex at the same time. The results demonstrate that FIS can effectively repair the hole in dental models with complex geometry feature. In the future, other related factors should be introduced into this research, such as the positional relationship of the adjacent vertex, space angle of the adjacent edge, normal angle of the adjacent surface.

Acknowledgment. This work is partially supported by the Education Department of Heilongjiang Province (Grant No. 135209243).

REFERENCES

[1] P. Buyssens, O. Le Meur, M. Daisy et al., Depth-guided disocclusion inpainting of synthesized RGB-D images, *IEEE Trans. Image Processing*, vol.26, no.2, pp.525-538, 2017.

[2] G. Luo and Y. Zhu, Foreground removal approach for hole filling in 3D video and FVV synthesis, *IEEE Trans. Circuits Syst. Video Technol.*, vol.27, no.10, pp.2118-2131, 2017.

[3] M. Ciotta and D. Androutsos, Depth guided image completion for structure and texture synthesis, *Proc. of IEEE Int. Conf. Acoust., Speech Signal Process.*, Shanghai, China, pp.1199-1203, 2016.

[4] J. Howard, B. Morse, S. Cohen and B. Price, Depth-based patch scaling for content-aware stereo image completion, *Proc. of IEEE Winter Conf. Appl. Comput. Vis.*, Steamboat Springs, USA, pp.9-16, 2014.

[5] H. G. Kim et al., Temporally consistent hole filling method based on global optimization with label propagation for 3D video, *Proc. of IEEE Int. Conf. Image Process.*, Quebec, Canada, pp.3136-3140, 2015.

[6] S. Li, C. Zhu and M.-T. Sun, Hole filling with multiple reference views in DIBR view synthesis, *IEEE Trans. Multimedia*, vol.20, no.8, pp.1948-1959, 2018.

[7] P. Horhaew and C. Sinthanayothin, Curvilinear hole filling for 3D digital dental models, *International Journal of Medical Engineering and Informatics*, vol.8, no.1, pp.76-84, 2016.

[8] M. A. Fortes, P. Gonzalez, A. Palomares et al., Filling holes with shape preserving conditions, *Mathematics & Computers in Simulation*, vol.118, pp.198-212, 2015.

[9] M. Centin, N. Pezzotti and A. Signoron, Poisson-driven seamless completion of triangular meshes, *Computer Aided Geometric Design*, vols.35-36, pp.42-55, 2015.

[10] G. Harary, A. Tal and E. Grinspun, Context-based coherent surface completion, *ACM Trans. Graphics*, vol.33, no.1, pp.57-76, 2014.

[11] P. Sahay and A. N. Rajagopalan, Geometric inpainting of 3D structures, *Proc. of the IEEE Conference on Computer Vision and Pattern Recognition Workshops*, Boston, MA, pp.1-7, 2015.

[12] Y. J. Liu, M. Wang et al., Strategy of classification and repairing for hole of incomplete point clouds based on fuzzy inference, *Journal of Computational and Theoretical Nanoscience*, vol.13, pp.8227-8233, 2016.